www.serd.ait.ac.th/reric

Pressure and Heat Transfer in Staggered Arrangement Circular Tubes with Airfoil Vortex Generator

M. Gorji-Bandpy*[1], S. Soleimani* and F. Hossein-Nejad*

Abstract – *In this paper the numerical solution of flow and heat transfer have been computed on staggered arrangement circular tubes and modeled by Navier-Stokes and energy equations. Two-dimensional flow, with Reynolds numbers between 100 to 500 is used. Flow is assumed to be incompressible, steady state and the thermo physical characteristics are constant. The elliptic differential equations are used to generate orthogonal grid and finite volume equations are solved to link pressure and velocity terms. Nusselt numbers, pressure changes, velocity and friction coefficients have been obtained in two conditions of with and without obstacle, and compared. The results show that the usage of airfoil obstacle is efficient for increasing heat transfer in spite of more friction coefficient and more pressure reduction.*

Keywords – Airfoil vortex generator, heat exchanger, heat transfer enhancement, numerical computation.

1. INTRODUCTION

Heat exchangers are used in a wide range of engineering applications, such as, power generation, auto and aerospace industry and electronics. An efficient heat exchanger in such systems could result in the lesser consumption of the energy resources, which provides both economical and environmental benefits. Increasing demands are being placed on heat exchanger performance for reasons of compactness, economy in manufacturing and operating costs, energy conservation and even for ecological reasons. The importance of these issues continues to motivate the study of enhancement techniques.

There are numerous ways to increase the heat transfer which include, treated surfaces, rough surfaces, extended surfaces, coiled tubes, surface vibration, fluid vibration and jet impingement. Another common method is to apply vortex generators (VG), such as ribs, wings and winglets.

Vortex generators, generate longitudinal vortices which swirl the primary flow and increase the mixing of downstream regions. In addition, the vortex generator determines the secondary flow pattern. Thus, heat transfer enhancement is associated with the secondary flow with relatively low penalty of pressure drop [1].

The first literature reporting the enhancement of heat transfer of using surface protrusion vortex generators is by [2]. They noted a maximum increase in the local Nusselt number of 40%. Eibeck and Eaton [3] conducted heat transfer measurement for a single longitudinal vortex embedded in a turbulent boundary layer. They interpreted their data in terms of vortex circulation and boundary layer thickness. Pauley and Eaton [4] extended this work to consider vortex pairs. Co-rotating pairs were observed to move together and coalesce into a single vortex as they were adverted downstream. Other numerical studies have investigated the flow past over heat exchanger especially flow past tube in a tube bundle by [5], [6] and [7].

Alessio and Dennis [8] investigated using elliptical tubes in heat exchangers in forced convection for low Reynolds numbers. Gorji-Bandpy *et al*. [9] investigated using elliptical vortex in heat exchangers with in-lined circular tubes for various Reynolds numbers. Kashevarov [10] reported the exact solution of forced convection problem in an elliptical cylinder. He considered a dominant potential flow around cylinder and solved analytically the two dimensional energy equations. One of the most important investigations about forced convection from a straight elliptical tube has been done by [11]. He studied on forced convection heat transfer of two dimensional laminar flow in a constant temperature elliptic tube across the uniform flow. Most of the investigation about using vortex generator obstacles in heat exchangers has been done on triangular obstacles and in some cases on rectangular obstacles [12]-[14].

Recent efforts have successfully utilized computational fluid dynamics (CFD) modeling to explain the fundamental principles behind the energy separation reduced by the vortex tube. Frohlingsdorf and Unger [15] modeled the flow within a vortex tube using a CFD solver that included compressible and turbulent effects. The numerical predictions qualitatively predicted the experimental results are presented by Bruun [16].

Ahlborn *et al.* [17], [18] show the dependence of vortex tube performance on normalized pressure drop with a numerical model. Aljuwayhel *et al*. [19] successfully utilized a CFD model of the vortex tube to understand the fundamental processes that drive the power separation phenomena.

Tsay *et al*. [20] numerically investigated the heat transfer enhancement due to a vertical baffle in a backward-facing step flow channel. The effect of the baffle height, thickness and the distance between the baffle and the backward facing step on the flow structure was studied in details for a range of Reynolds number varying from 100 to 500.They found that an introduction of a baffle into the flow could increase the average Nusselt number by 190%. They also observed that the flow conditions and heat transfer characteristics are strong

* Department of Mechanical Engineering, Mazandaran University, P.O. Box 484, Babol, Iran.

[1] Corresponding author;
E-mail: gorjibandpy@yahoo.com.

function of the baffle position. Tiwari *et al.* [21] numerically simulated the effect of the delta winglet type vortex generator on flow and heat transfer in a rectangular duct with a built-in circular tube. They observed that the vortices induced by the vortex generator resulted in an increase in the span-averaged Nusselt number at the trailing edge of the vortex generator by a factor of 2.5 and the heat transfer enhancement of 230% in the near wake region. Lin and Jang [22] numerically studied the performance of a wave-type vortex generator installed in a fin-tube heat exchanger. They found that an increase in the length or height of the vortex generator increases the heat transfer, as well as the friction losses. They reported up to 120%increase in the heat transfer coefficient at a maximum area reduction of 20%, accompanied by a 48%increase in the friction factor.

In this paper the usage of airfoil obstacle in heat exchanger is numerically studied. A numerical solution based on the finite volume method was carried out on the steady laminar heat transfer in hydrodynamically developed but thermally developing flows. The main aim of the present research is to propose a novel strategy that can augment heat transfer but nevertheless can reduce pressure-loss in a fin-tube heat exchanger with circular tubes in a relatively low Reynolds number flow, by deploying airfoil winglet-type vortex generators. The complete Navier–Stokes equations together with the energy equation have been solved to obtain a detailed analysis of the flow structure together with heat transfer characteristics of the proposed configuration for the finned circular tube heat exchangers.

2. GOVERNING EQUATIONS

The governing equations are the mass, momentum and energy equations which were simplified in accordance with the assumptions of two dimensional incompressible steady state flows with constant properties, for a Newtonian fluid:

$$\frac{\partial u_i}{\partial x_i} = 0.0 \qquad \text{(i=1, 2)} \tag{1}$$

$$\frac{\partial (u_i, \phi)}{\partial x_i} = \frac{\partial}{\partial x_i}\left(\Gamma_\phi \frac{\partial \phi}{\partial x_i} \right) + S_\phi \tag{2}$$

In these equations, ϕ is a general dependant variable, Γ_ϕ is diffusion coefficient and S_ϕ is the source term that two latter values are dependant on ϕ. The ϕ dependant variable is used instead of velocity and temperature in equation. So, above equations is rewritten into non-dimensional groups as follows:

$$\frac{\partial u}{\partial x} + \frac{\partial v}{\partial y} = 0 \tag{3}$$

$$\frac{\partial (uv)}{\partial x} + \frac{\partial (uv)}{\partial y} = -\frac{\partial p}{\partial x} + \frac{1}{Re}\left(\frac{\partial^2 u}{\partial x^2} + \frac{\partial^2 v}{\partial y^2} \right) \tag{4}$$

$$\frac{\partial (uv)}{\partial x} + \frac{\partial (uv)}{\partial y} = \frac{\partial p}{\partial y} + \frac{1}{Re}\left(\frac{\partial^2 u}{\partial x^2} + \frac{\partial^2 v}{\partial y^2} \right) \tag{5}$$

$$\frac{\partial (uT)}{\partial x} + \frac{\partial (vT)}{\partial y} = \frac{1}{Re.Pr}\left(\frac{\partial^2 T}{\partial x^2} + \frac{\partial^2 T}{\partial y^2} \right) \tag{6}$$

Dimensionless parameters are carried out as follows:

$$x^* = \frac{X}{L} \tag{7}$$

$$y^* = \frac{y}{L} \tag{8}$$

$$v^* = \frac{v}{u_\infty} \tag{9}$$

$$u^* = \frac{u}{u_\infty} \tag{10}$$

(Note: Star symbol has been omitted in above equations)

Where L is specified length, ρ_∞ is density, u_∞ is velocity, T_∞ is base temperature and is wall temperature. Dimensionless numbers are described as follows:

$$Re = \frac{\rho_\infty . u_\infty . L}{\mu_\infty} \tag{11}$$

$$Pr = \frac{\mu . c}{k} \tag{12}$$

$$Nu = \frac{hL}{k} \tag{13}$$

By applying general units of boundary fitted smooth line, it must be a conversion from physical domain into computational domain.

For studying the effect of pressure losses at airfoil obstacle after heat exchanger's tubes, the pressure coefficient must be calculated as follows:

$$Cp = \frac{\Delta p}{\rho u^2 / 2} \tag{14}$$

For the numerical method which is used in this work the discrete equations are obtained by integrating from the governing equations into the control volume (finite volume) which the details are presented by [23].

The discrete algorithm for pressure equation, pressure-velocity coupling, momentum equation and energy equation are STANDARD, SIMPLE, FIRST ORDER UPWIND and FIRST ORDER UPWIND algorithm respectively.

3. GEOMETRY AND BOUNDARY CONDITIONS

Most of the complex heat exchangers use circular section tubes. In this study, the heat exchanger with circular tubes considered and there is airfoil obstacle with angle of 45 degree with horizontal between tubes. The tubes with airfoil obstacle are shown schematically in Figure 1. For obtaining better results, preceding and following edge of obstacle, is completely considered aerodynamically and as far as governing equations on flow are concern, the whole boundary condition must be known.

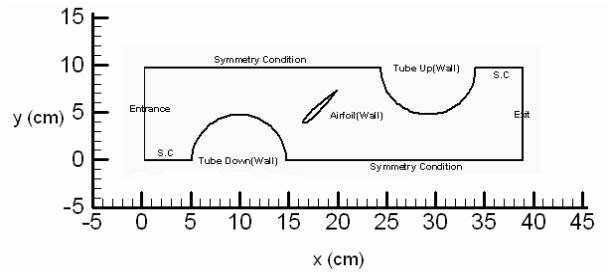

Fig. 1. Schematically view of tube with airfoil obstacle.

Inlet (X=0)

Profiles of velocity, pressure and temperature are known in inlet border. At the inlet, a constant stream wise velocity has been used with other velocities being set to zero and the temperature distribution is constant.

$$U = u_{in} \tag{15}$$

$$V = 0 \tag{16}$$

$$P = p_{in} \tag{17}$$

$$T = T_{in} \tag{18}$$

Outlet (X=L)

At outlet, due to the existence of the Neumann boundary conditions that are used for all variables, the stream wise variable gradients are set to be zero [23]:

$$\frac{\partial u_i}{\partial x} = 0.0 \tag{19}$$

$$\frac{\partial P}{\partial x} = 0.0 \tag{20}$$

$$\frac{\partial T}{\partial x} = 0.0 \tag{21}$$

Lateral Boundaries (y=0, y=H)

At lateral boundaries, we will apply the symmetrical condition by boundary fitted conditions. In this condition, the net passing flow through the symmetric line is equal to zero. So the velocity component that is vertical by boundary is set zero and gradient of other variables are also zero:

$$\frac{\partial u}{\partial y} = 0.0 \tag{22}$$

$$\frac{\partial P}{\partial y} = 0.0 \tag{23}$$

$$\frac{\partial T}{\partial y} = 0.0 \tag{24}$$

$$V = 0.0 \tag{25}$$

Solid Wall

The no-slip boundary conditions have been used and therefore velocity components are set to be zero and also temperature distribution on the wall is considered constant.

$$U = 0 \tag{26}$$

$$V = 0 \tag{27}$$

$$T_{tube} = T_{wall} = const. \tag{28}$$

In addition, by dividing the computational model into sub-domains obtained numerical values can be substituted.

4. RESULTS AND DISCUSSIONS

In this section we will show the graphs of Nusselt numbers, pressure and velocity around underneath and upper tube at Reynolds number equals to 350 as well as the graphs of Nusselt number, friction coefficient (c_f) and stream function against various Reynolds numbers for both cases of with airfoil obstacle and without airfoil obstacle.

In Figure 2, a comparison between two grid solution results for different Nusselt numbers was first conducted. This was done to ensure that the prediction made with this work is trustworthy. The results indicate that the comparisons between two grids are in a good agreement for different Nusselt numbers against various Reynolds numbers.

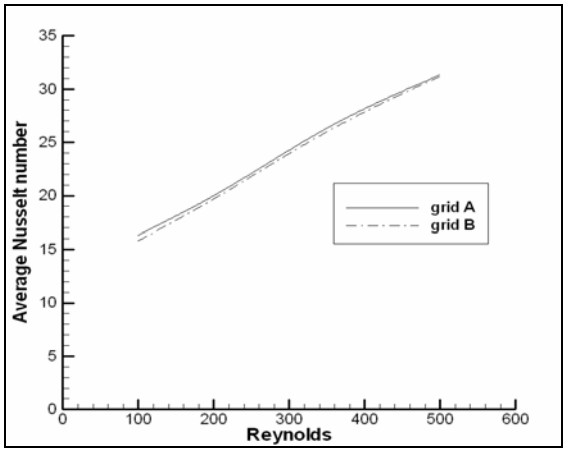

(a)

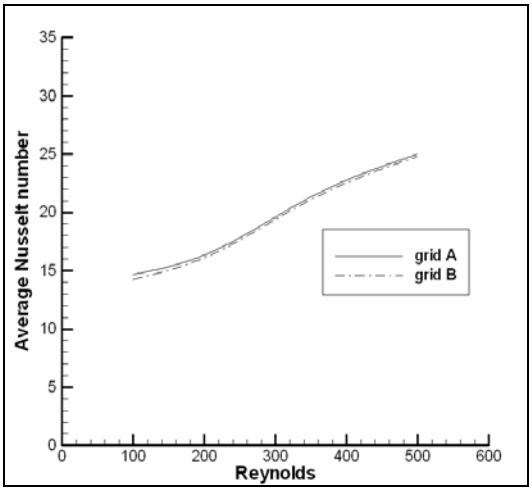

(b)

Fig. 2. Average Nusselt number against various Re number for grid A (10514 elements) and grid B (30810 elements) for (a) with obstacle and (b) without obstacle case.

Figure 3 shows the variation of local Nusselt numbers distributed around the tube of heat exchanger for both cases of with and without obstacle.

In Figure 3a the Nusselt number increase is observed almost around of underneath tube for with obstacle case. Since in the case of without obstacle there is a vortex at the rear of underneath tube, as shown in (Figure 4c) the Nusselt number is lower than in the case with obstacle which there is no vortex at the rear of the that tube, (Figure 4d). Furthermore in the case of with obstacle an increase in velocity at the rear of that tube is seen which causes the increase of heat transfer coefficient.

In Figure 3b for the case of with obstacle due to vorticity, as shown in Figure 4c the lower Nusselt number is observed than the case of without obstacle, Figure 4d. Furthermore the velocity of flow around the upper tube in the case of with obstacle is lower than in the case of without obstacle which decreases the heat transfer coefficient.

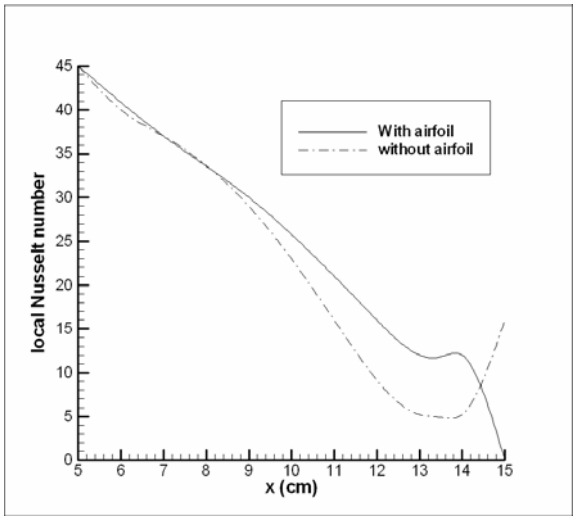

(a)

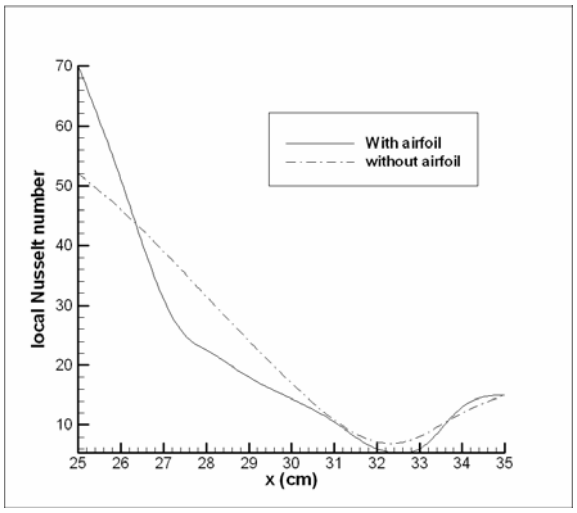

(b)

Fig. 3. Variations of local Nusselt number for with and without airfoil obstacle case distributed around the (a) underneath and (b) upper tube, at Re=350.

Figures 4a to 4f shows the stream function for with and without obstacle case at different Reynolds numbers of 200,350 and 500 respectively.

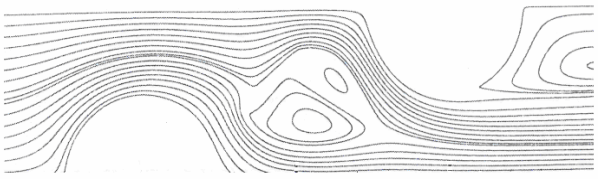

Fig. 4a. Stream function for with obstacle case, at Re=200.

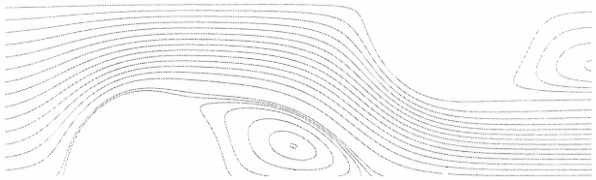

Fig. 4b. Stream function for without obstacle case, at Re=200.

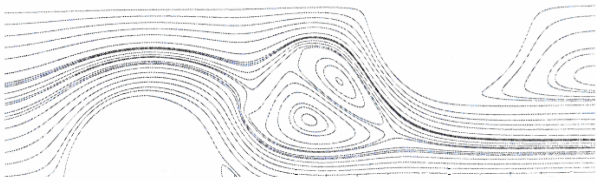

Fig. 4c. Stream function for with obstacle case, at Re=350.

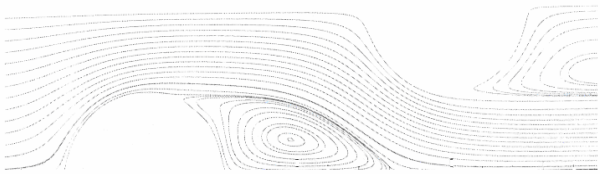

Fig. 4d. Stream function for without obstacle case, at Re=350.

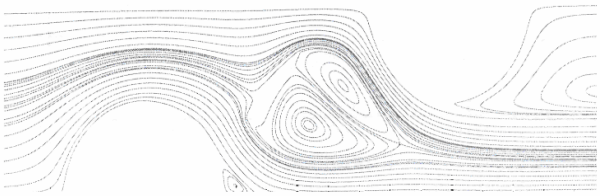

Fig. 4e. Stream function for with obstacle case, at Re=500.

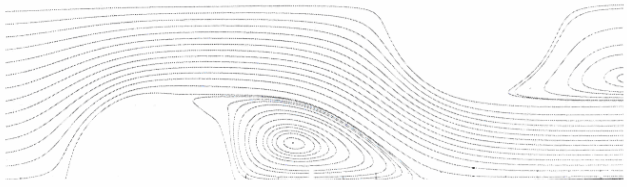

Fig. 4f. Stream function for with obstacle case, at Re=500.

Figure 5 shows the variations of pressure distributed around the tube of heat exchanger for both cases of with and without obstacle. In this figure, because of the obstacle, an increase in pressure is seen for underneath tube in with obstacle case. Although because of pressure drop which is a sensible result of obstacle there is a pressure reduction for upper tube in with obstacle case.

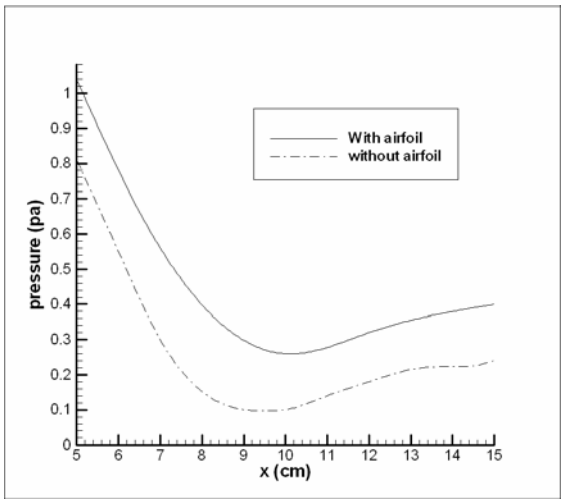

(a)

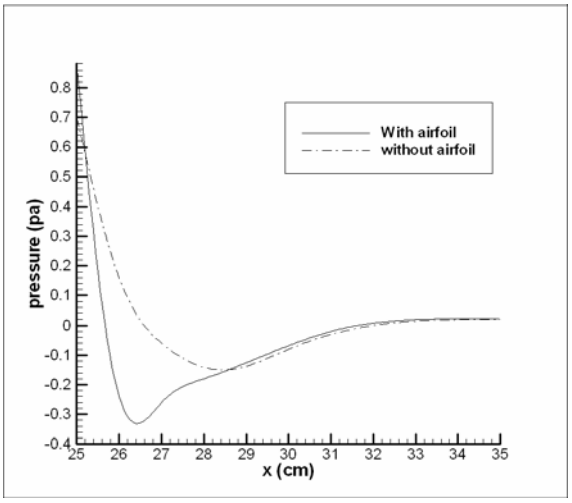

(b)

Fig. 5. Variations of pressure for with and without airfoil obstacle case distributed around the (a) underneath and (b) upper tube, at Re=350.

Figure 6 shows the variations of velocity distributed around underneath and upper tube for with and without obstacle case at Reynolds equal to 350.

Figure 7 shows the variation of Nusselt numbers against Reynolds numbers for both cases of with and without airfoil obstacle.

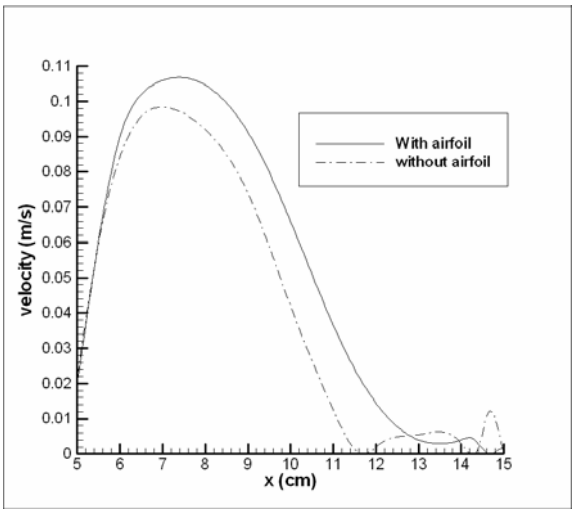

(a)

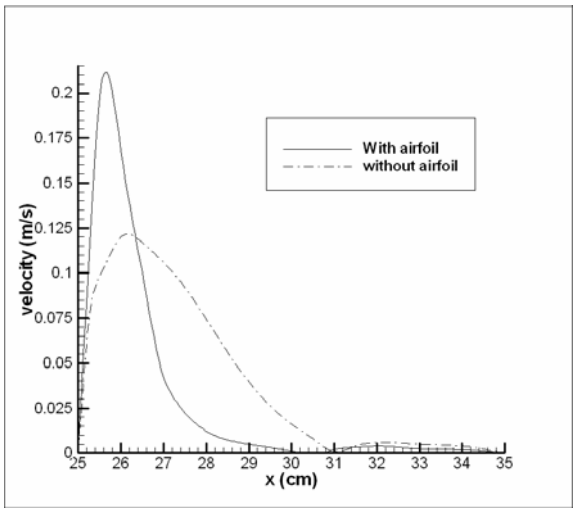

(b)

Fig. 6. Variations of velocity for with and without airfoil obstacle case distributed around the (a) underneath and (b) upper tube, at Re=350.

The ascendant trend of Nusselt number in this figure for with and without obstacle case is because of the increase in Reynolds number, velocity of flow and therefore the heat transfer coefficient of fluid. The reason of increase in difference of Nusselt numbers between with and without obstacle case can be justified. Because of increasing of Reynolds numbers, the vortex at the rear of obstacle grows and this leads to the faster movement of the flow around the tubes, as shown in Figures 4a to 4f and therefore the heat transfer coefficient increases.

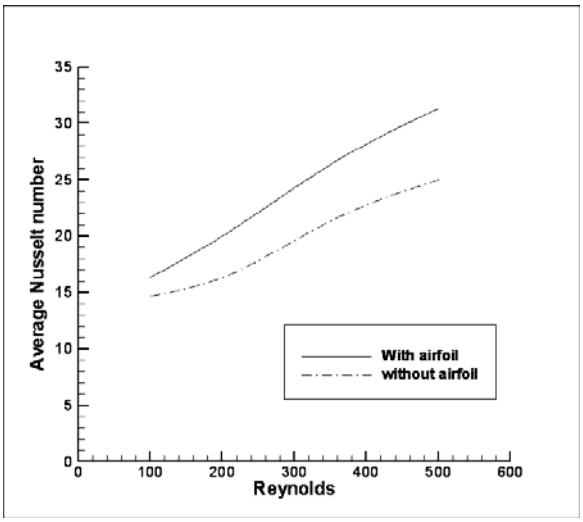

Fig. 7. Variations of average Nusselt number against Reynolds number for with and without airfoil obstacle.

Figure 8 shows the variation of friction coefficient (c_f) against Reynolds numbers for both cases of with and without airfoil obstacle. As this figure indicates, by increasing Reynolds number the friction coefficient (c_f) for both cases of with and without obstacle increases, whereas in the case of with obstacle the more value of c_f is observed.

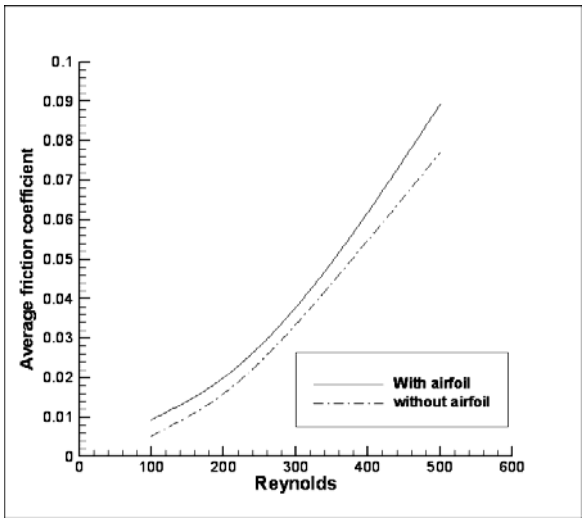

Fig. 8. Variation of c_f against Reynolds numbers for with and without airfoil obstacle.

Figure 9 shows the variation of Nusselt numbers as well as pressure drop against various angles of attack for just with obstacle case. As the Figure 9a indicates the average Nusselt number rapidly increases from 0 degree to 45 degree angles of attack and gradually from 45 degree to 90 degree of angles of attack .On the other hand, as Figure 9b shows the pressure difference between the inlet and outlet flow (Δp), increases gradually from 0 degree to 45 degree of angles of attack and rapidly from 45 degree to 90 degree of angles of attack. As a result the optimum value of angles of attack is equal to 45 degree which is in accordance with high Nusselt number and low pressure drop.

Figure 10 shows the variation of pressure difference between the inlet and outlet flow against various Reynolds numbers for both cases of with and without obstacle.

As the figure shows, by increasing the Reynolds numbers the value of pressure difference between the inlet and outlet flow (Δp) increases rapidly.

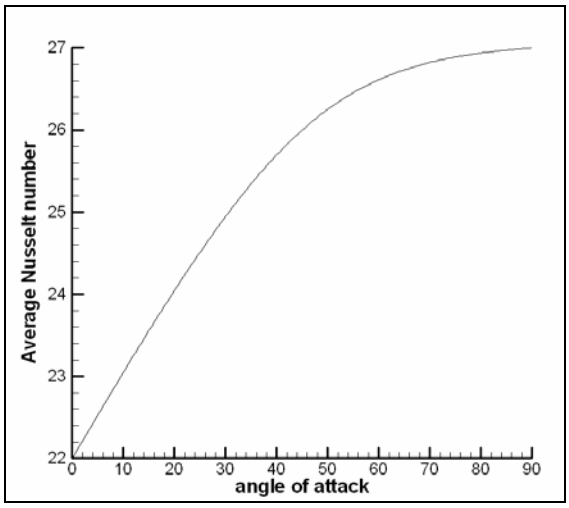

(a)

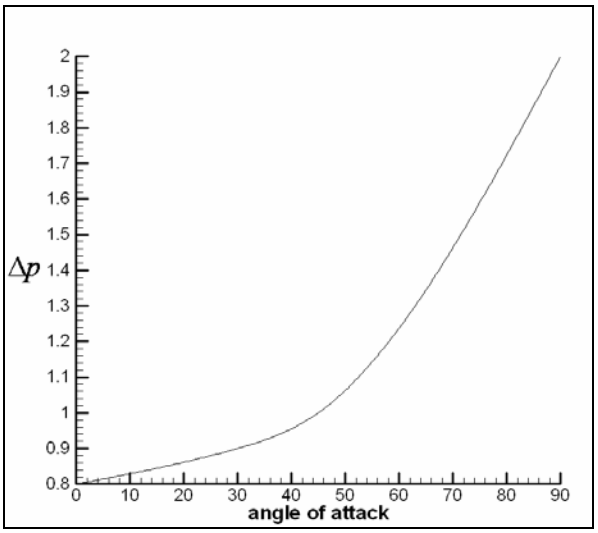

(b)

Fig. 9. (a)Variation of average Nusselt numbers against various angles of attack, degree (b) variation of pressure difference between the inlet and outlet flow (Δp) against various angles of attack, degree for with obstacle case

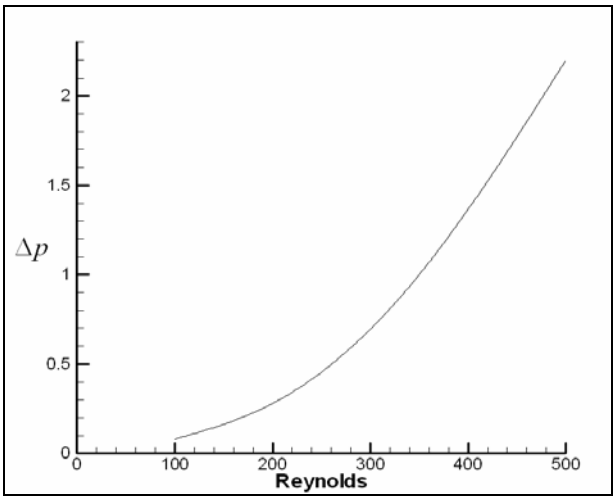

(a)

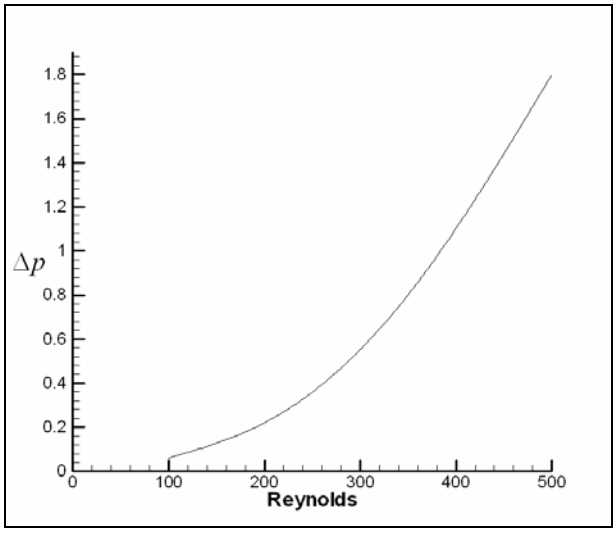

(b)

Fig. 10. Variation of pressure difference between the inlet and outlet flow (Δp) against various Re numbers for the case of (a) with obstacle and (b) without obstacle.

5. CONCLUSION

Heat exchangers are used in a wide range of engineering applications, such as, power generation, auto and aerospace industry and electronics. An efficient heat exchanger in such systems could result in the lesser consumption of the energy resource, which provides both economical and environmental benefits**.** There are many concepts for improving the performance of heat exchangers by replacing the circular tubes with oval tubes and adding strategically located vortex generators. Theoretical background and experimental results are main reasons for attention to these approaches. In this paper the numerical solution of flow and heat transfer have been computed on staggered arrangement circular tubes and modeled by Navier-Stokes and energy equations.

The results reveal that in the case of heat exchanger with airfoil obstacle, the values of Nusselt numbers for the tubes are mostly higher than those of the tubes without obstacle. According to the results, it is clear that the more Reynolds number, the better effect it has and the average Nusselt numbers increase with presence of airfoil obstacle case about 20 to 30 % with a penalty increase in friction coefficient (c_f) of 10 to 15 %.

The local Nusselt numbers prediction for laminar flow of Newtonian fluids around the obstacle of heat exchanger is studied. The momentum and energy balance equations have been written in terms of dimensionless quantities. A numerical solution based on the finite volume method was carried out on the steady laminar heat transfer in hydrodynamically developed but thermally developing flows. The local Nusselt numbers and pressure in entrance region are numerically calculated and shown in graphs as a function of length of tubes and compared with the well established results. At last the values of the average Nusselt numbers and friction coefficient (c_f) against various Reynolds number are presented. It is concluded that the average Nusselt number increase with presence of airfoil obstacle and the usage of these obstacles is efficient for increasing heat transfer in spite of more friction coefficient and more pressure reduction.

It is obvious that by adding vortex generator in the heat exchanger the cost of manufacturing the heat exchanger increases but this increase in cost is really less than the saving money by saving energy because of the usage of the heat exchanger with higher efficiency.

NOMENCLATURE

C	Heat capacity ($j/kg.k$)
C_p	Pressure coefficient
H	Channel height (m)
c_f	Friction coefficient
k	Thermal conductivity coefficient ($j/m.k$)
L	Length (m)
Nu	Nusselt number
P	Pressure (Pa)
Pr	Prandtl number (ν/α)
Re	Reynolds number ($\rho u_\infty L/\mu$)
T	Temperature ($^\circ c$)
T_w	Wall temperature ($^\circ c$)
U	Horizontal contra variant velocity component ($m.s^{-1}$)
u	Horizontal Cartesian velocity component ($m.s^{-1}$)
V	Vertical contra variant velocity component ($m.s^{-1}$)
v	Vertical Cartesian velocity component ($m.s^{-1}$)
x,y	Cartesian coordinates

Greek Letters

Γ_ϕ	Diffusion coefficient
ΔP	Pressure loss **(**pa)
μ	Dynamic velocity of fluid
ρ	Density (kg/m^3)
ϕ	General variable
S_ϕ	Source term

Subscripts

i	Covariant vector
in	Inlet characteristic of fluid
tube	Characteristic of tube
∞	Free stream

Superscripts

*Non dimensional

REFERENCES

[1] Jacobi, A.M., and Shah, R.K. 1995. Heat transfer surface enhancement through the use of longitudinal vortices. *Experimental Thermal. Fluid Science*. 11: 295–309.

[2] Edwards, F.J., and Alker, G.J.R. 1974. The improvement of forces convection surface heat transfer using surfaces protrusions in the form of (A) cubes and (B) vortex generators. In *Proceedings of the 5th International Conference on Heat Transfer* Tokyo, 2: 244–248.

[3] Eibeck, P.A., and Eaton, J.K. 1987. Heat transfer effects of a longitudinal vortex embedded in a turbulent boundary layer. ASME *Journal of Heat Transfer* 109: 37–57.

[4] Pauley, W.R., and Eaton, J.K. 1988. Experimental study of the development of longitudinal vortex pairs embedded in a turbulent boundary layer. *AIAA Journal* 26: 816–823.

[5] Sparrow, E.M., and Liu, C.H. 1979. Heat transfer, pressure drop and performance relationships for in-line, staggered, and continues plate heat exchangers. *International Journal of Heat and Mass Transfer* 22: 1613-1626.

[6] Kundu, D., Haji-Sheikh, A., and Lou, D.Y.S. 1991. Pressure and heat transfer in cross flow over cylinders between two parallel plates. *International Journal of Heat and Mass Transfer* 19: 345-360.

[7] Buyruk, E., Johnson, B.W., and Owen, I. 1998. Numerical and experimental study of flow and heat transfer around a tube in cross-flow at low Reynolds number. *International Journal of Heat and Fluid flow* 19: 223-232.

[8] Alessio, S.J.D. and Dennis, S.C.R. 1995. Steady laminar forced convection from an elliptic cylinder. *Engineering Mathematics* 29: 181-193.

[9] Gorji-Bandpy, M., Mohseni, L., and Jannat-Abadi, E.M. 2006. A numerical investigation of a two dimensional flow in in-lined circular tubes with elliptic vortex generator. *Heat Transfer*. The New Forest, U.K., 2: 151-158.

[10] Kashevarov, A.V. 1996. Exact solution of the problem of convective heat transfer for an elliptic cylinder and a plate in a fluid with small Prandtl number. *Fluid Dynamics* 31: 356-360.

[11] Badr, H.M. 1998. Forced convection from a straight elliptical tube. *Heat and Mass Transfer* 34: 229-236.

[12] Sheng, L.J., Wu, Y.H., and Jang, J.Y. 2004. Heat transfer and fluid flow analysis in plate-fin and tube heat exchangers with a pair of block shape vortex generators. *International Journal of Heat and Mass Transfer* 47: 4327-4338.

[13] Kwak, K.M., Torii, K., and Nishino, K. 2005. Simultaneous heat transfer enhancement and pressure loss reduction for finned-tube bundles with the first or two transverse rows of built-in winglets", *Experimental Thermal and Fluid Science* 29(5): 625-632.

[14] Torii, K., Keak, K.M., and Nishino, K. 2002. Heat transfer enhancement accompanying pressure-loss reduction with winglet-type vortex generators for fin-tube heat exchangers. *International Journal of Heat andMass Transfer* 45(18): 3795-3801.

[15] Frohlingsdorf, W., and Unger, H. 1999. Numerical investigations of the compressible flow and the energy separation in the Ranque–Hilsch vortex tube. *International Journal of Heat and Mass Transfer* 42: 415–422.

[16] Bruun, H.H. 1969. Experimental investigation of the energy separation in vortex tubes. *Journal of Mechanical Engineering Science*. 11(6): 567–582.

[17] Ahlborn, B., Keller, J.U., Staudt, R., Treitz, G., and Rebhan, R. 1994. Limits of temperature separation in a vortex tube *Journal of Physic D, Applied Physics* 27: 480–488.

[18] Ahlborn, B., Camire, J., and Keller, J.U., 1996. Low-pressure vortex tubes. *Journal of Physic D, Applied Phyics* 29: 1469–1472.

[19] Aljuwayhel, N.F., Nellis, G.F., and Klein, S.A. 2005. Parametric and internal study of the vortex tube using a CFD model. *International Journal of Refrigeration* 28(3): 442–450.

[20] Tsay, Y.L., Chang, T.S., and Cheng, J.C. 2005. Heat transfer enhancement of backward-facing step flow in a channel by using baffle installed on the channel wall. *ACTA. Mechanics* 174: 63-76.

[21] Tiwari, S., Prasad, P.L.N., and Biswas, G. 2003. A numerical study of heat transfer fin tube heat exchangers using winglet-type vortex generators in common flow down configuration. *Progress in Computational Fluid Dynamics* 3:32 -41.

[22] Lin, C.N., and Jang, J.Y. 2002. Conjugate heat transfer and fluid flow analysis in fin tube heat exchangers with wave-type vortex generators. *Journal of Enhanced Heat Transfer* 9: 123-36.

[23] Anderson, A. and David, J. 1995. Computational Fluid Dynamics. *McGraw-Hill, Inc*. 23-43.